Characterization of Calcium-Deficient Hydroxyapatite after a Catalytic Reaction with Trichloroethylene Vapor

Harumitsu NISHIKAWA,* Shigero IKEDA,† and Hideki MONMA††
Gifu Prefectural Research Institute for Environmental Pollution, 8-58-2, Yabuta, Gifu 500
†Department of Materials Chemistry, Faculty of Science and Technology, Ryukoku University, 1-5, Yokotani, Oe-cho Seta, Otsu, Shiga 520-21
††National Institute for Research in Inorganic Materials, 1-1, Namiki, Tsukuba, Ibaraki 305

(Received March 17, 1993)

Calcium-deficient hydroxyapatite (DAp) was characterized both before and after an oxidative catalytic reaction with trichloroethylene (TCE) vapor at 450 °C. Most of the Cl in the TCE which decomposed by the reaction was captured as Cl^- in DAp. This result supports the assumption reported in a previous paper. On the basis of infrared spectroscopic and X-ray photoelectron spectroscopic results, the captured Cl species was assumed to replace OH^- in DAp and to form chloroapatite.

The environmental contamination of trichloroethylene (TCE) is a serious problem due to its harmfulness to human health. Still, TCE is widely used as a superior solvent or cleaning material in various industries. The various decomposition procedures, such as multi catalytic combustion[1] and catalytic destruction,[2—4] have been studied for gaseous compounds, such as TCE and related chlorinated organic compounds. In a previous paper[5] we reported on a simple and effective decomposition procedure for TCE vapor using calcium-deficient hydroxyapatite (referred to as DAp).

DAp having the composition $Ca_{10-z}(HPO_4)_z(PO_4)_{6-z}(OH)_{2-z}\cdot nH_2O$ $(0<z\leqq 1)$ is known as a catalytic material for phenol synthesis[6—8] as well as the dehydration and dehyrogenation of alcohols.[9,10] The decomposition of TCE vapor over DAp at 400—500 °C in the presence of H_2O and O_2 is given by

$$CHCl{=}CCl_2 + H_2O + O_2 \rightarrow CO + CO_2 + 3HCl.$$

It was assumed that any produced HCl was immediately captured by DAp, since little HCl was detected in the effluent gas.

This paper reports on the characterization of the Cl species captured and the surface variation of DAp after the oxidative catalytic decomposition of TCE.

Experimental

The apparatus used for the TCE reaction over DAp and its experimental conditions were described in a previous paper.[5]

The Ca/P molar ratio of DAp used was 1.54, and the BET surface area was 53 $m^2\,g^{-1}$. The catalytic decomposition of TCE was conducted by passing TCE vapor (60.7 ppm v/v) with air at 0.3 $dm^3\,min^{-1}$ through a 0.5 g bed of the DAp catalyst packed in a glass tube reactor with an inner diameter of 6 mm at 450 °C. The reaction was continued until the decomposition of TCE decreased to 20%.

Fresh and reacted DAp samples were analyzed by various methods, as follows: Cl^- amounts in DAp were determined by ion chromatography using a Yokogawa Electric Model IC7000, after dissolution with 1 M HNO_3 (1 M=1 mol dm^{-3}) and dilution with distilled water.

The X-ray powder diffraction (XRD) patterns were recorded on a Philips PW1700 diffractometer. The fourier transform infrared (FTIR) spectra were measured with a Shimadzu 8100 equipped with a diffuse reflectance spectroscope (DRS). The X-ray photoelectron spectra (XPS) were measured with a Shimadzu ESCA 100S using an X-ray power of 10 kV–3 mA (Mg). A depth analysis was carried out by ion etching (Ar: 2 kV–20 mA, 60 and 120 s) at spatter speed of about 25 A min^{-1}. The Cl contents in both surface and bulk portion of DAp were measured with an Akashi ISI-DS130 scanning electron microscope (SEM) equipped with a Philips 9900-ECON3 energy-dispersive X-ray spectroscope (EDX).

Results and Discussion

XRD and FTIR Characteristics. The XRD patterns of DAp samples both before and after the reaction with TCE were almost coincident with each other; the basic apatitic structure was therefore maintained before and after the reaction. Although the DAp after the reaction contained comparative amounts of Cl (as described below), no detectable shifts of the XRD peaks were observed, since the crystallinity of the DAp was low. The FTIR (DRS) spectra after a Kubelka-Munk conversion are shown in Fig. 1. The characteristic bands for the OH^- and $P_2O_7^{4-}$ groups in DAp appear at around 3570 and 730 cm^{-1}, respectively. The $P_2O_7^{4-}$ forms over 250 °C as follows:[13]

$$HPO_4^{2-} \rightarrow 1/2P_2O_7^{4-} + 1/2H_2O.$$

Though a band due to the apatitic OH^- was thought to appear at 3570 and 3495 cm^{-1} with some Cl^- substitution for OH^-,[11] the latter peak was not observed. On the other hand, the absorbance of the apatitic OH group after the reaction decreased to 65%, compared with that of fresh DAp. Since DAp after blank heating without TCE showed no change in the intensity of the absorbance of OH, the apatitic OH must participate in the capture of Cl. No other differences in the FTIR bands of DAp before or after the reaction were observed.

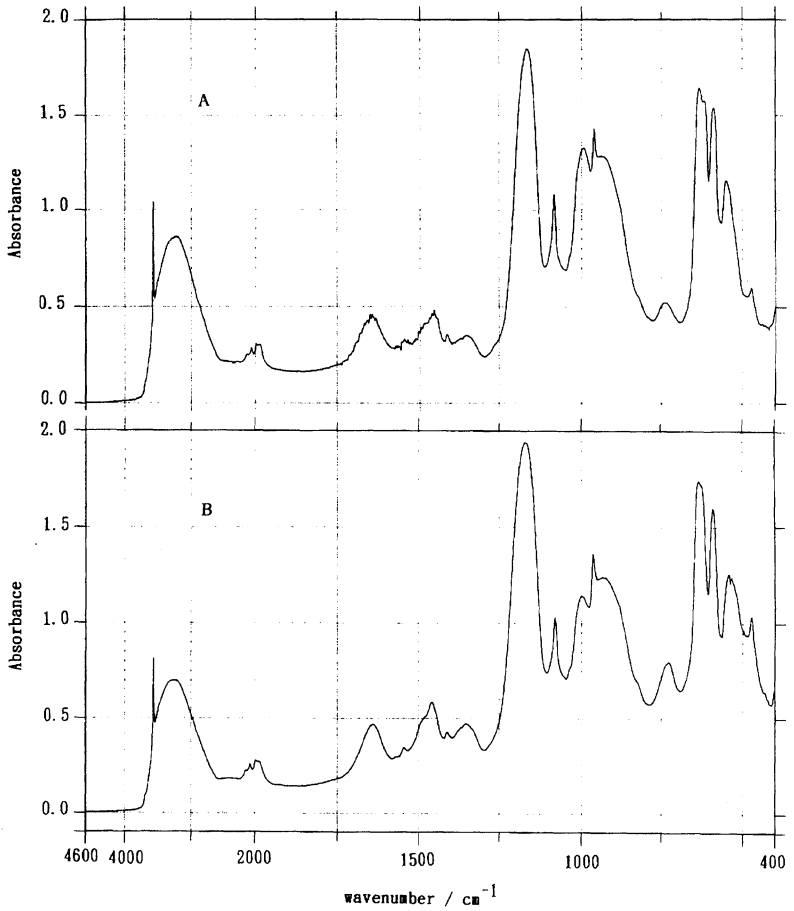

Fig. 1. FTIR spectra of fresh and reacted DAp. A: fresh DAp, B: DAp reacted with TCE.

Cl^- Amounts in DAp after a Catalytic Decomposition of TCE. The Cl^- amounts in fresh and reacted DAp are shown in Table 1. The Cl^- amount in DAp after the reaction was 85% of the total Cl amount in decomposed TCE. No Cl^- in DAp before the reaction was confirmed to have been detected. These results support the assumption that most of the Cl in decomposed TCE was fixed in DAp without volatilization as HCl.

Surface Characterization by XPS. The XPS data of both fresh and reacted DAp with TCE and synthetic chloroapatite are shown in Fig. 2 (A—C). The binding energies observed to the C 1s at 285.0 eV are listed in Table 2. The binding energies of Ca $2p_{3/2}$ and P2p of both fresh and reacted DAp are consistent with the reported values of hydroxyapatite.[12] Therefore, the surface apatitic structure seems to remain basically unchanged by the reaction. No difference in the depth analysis data was observed.

The quantitative data for Cl are shown in Table 3. Cl was detected only in the reacted DAp. Almost the same concentration of Cl was obtained for the different depth layers. The binding energy of Cl $2p_{3/2}$ (199.1 eV) observed after the reaction almost agreed with that of chloroapatite, and their spectrum shapes were very similar to each other. This energy value is also similar to the Cl $2p_{3/2}$ binding energy (199 eV) of $CaCl_2$.[12] However, when the reacted DAp was washed with distilled water, no Cl^- was detected in the solution by ion chro-

Table 1. Cl^- Amounts in Fresh and Reacted DAp[a)]

	Cl^-/DAp (mg g^{-1})		A/B[c)]	Cl/Ca
	(A) Found	(B) Calcd[b)]	(%)	molar ratio
Fresh	None	—	—	—
Reacted	13.3	15.8	85	0.045

a) Reaction conditions: TCE; 60.7 ppm (v/v), TCE reacted; 9.8 mg, DAp; 0.5 g, reaction temperature; 450 °C. b) Theroretical amount when the DAp was completely chlorinated with TCE reacted. c) Cl^- amount in DAp to Cl amount in decomposed TCE.

Table 2. Binding Energies of the Elements in DAp and Chloroapatite

	Binding energy (eV)		
	DAp		Chloroapatite
Element	Fresh	Reacted	
Ca $2p_{3/2}$	347.6	347.5	347.8
P 2P	133.5	133.5	133.6
Cl $2p_{3/2}$	—	199.1	199.3

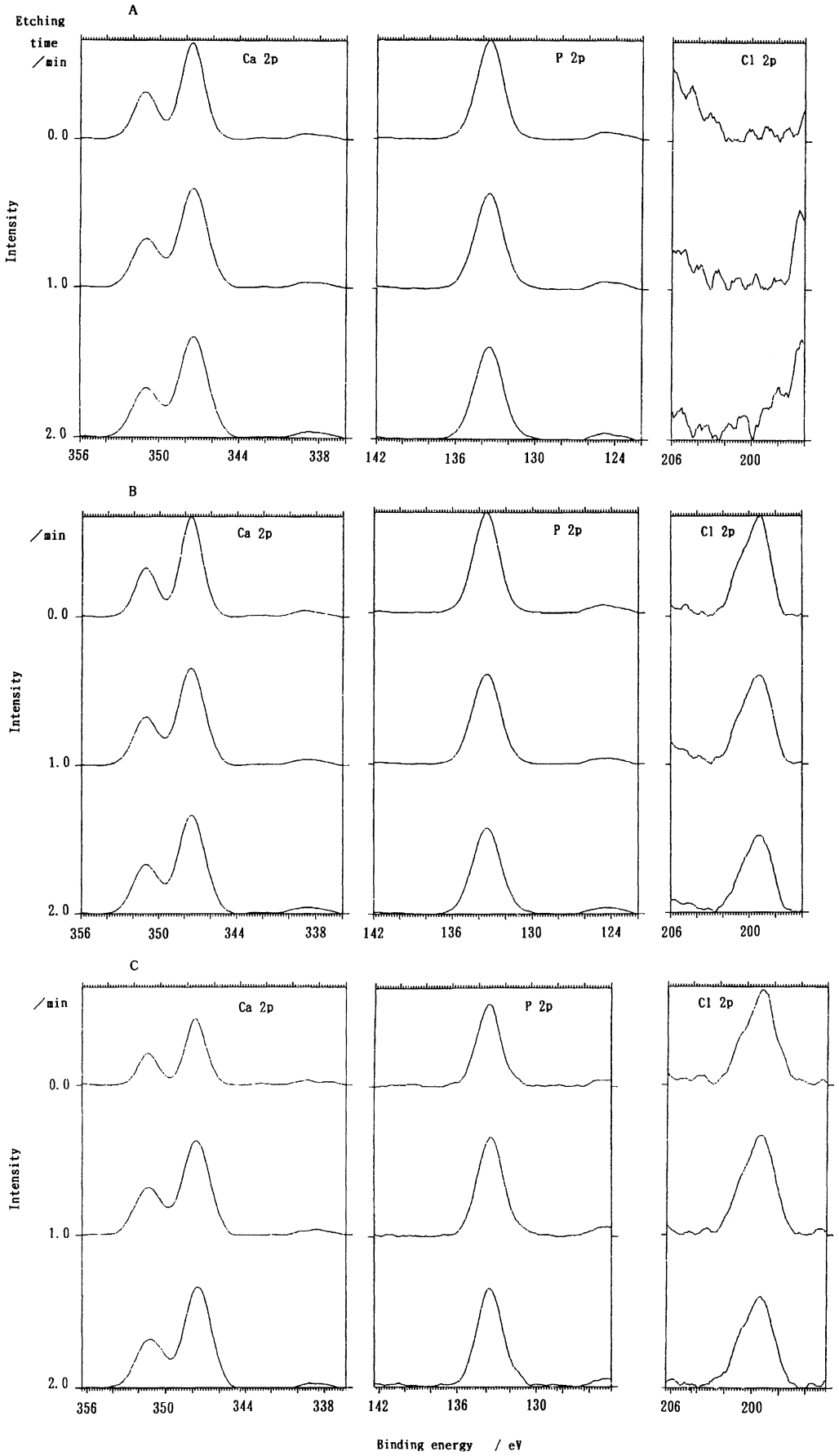

Fig. 2. XPS spectra of fresh, reacted DAp and chloroapatite. A: fresh DAp, B: DAp reacted with TCE, C: chloroapatite.

Table 3. Cl Concentration in Fresh and Reacted DAp by XPS

	Cl concentration[a] (molar %)	
	Fresh	Reacted
Layer 1	0.0	1.2
Layer 2	0.0	1.2
Layer 3	0.0	1.0

a) Cl concentration was calculated from relative peak area of Ca, P, O, and Cl. Layer 1; surface, Layer 2; etching time, 60 s, Layer 3; etching time, 120 s.

matography. It was therefore unreasonable that the Cl species in the DAp surface after the reaction was $CaCl_2$. The Cl species in the reacted DAp surface is in the form of chloroapatite.

EDX Analysis of the Surface and Bulk Portions of a DAp Particle. The Cl/Ca molar ratios on the surface and in a bulk portion of a DAp particle after the reaction were examined by EDX. The results are given in Table 4. No significant difference in the Cl/Ca molar ratio was observed between the surface and bulk portion. This fact suggests that the DAp particle was porous and that the Cl^- formed from TCE penetrated easily into the bulk.

The Cl/Ca molar ratio for the particle was higher than the value given in Table 1, showing an average value for the particles. This difference suggests that DAp particles packed in the reaction tube were not exposed homogeneously to the reactant TCE vapor.

Structure and Mechanism. An analysis of Cl^- in DAp after a reaction with TCE supported the idea that the major part of Cl in decomposed TCE is captured by DAp as the Cl^- species in the TCE/DAp oxidative catalytic decomposition. Since the Ca/P molar ratio of the DAp used in our experiment was 1.54, the DAp used is formulated as

$$Ca_{9.24}(HPO_4)_{0.76}(PO_4)_{5.24}(OH)_{1.24}.$$

The Cl/Ca molar ratio of the DAp after the TCE/DAp reaction was 0.045, as shown in Table 1. If the OH groups in DAp were exchanged by Cl from TCE, the composition of DAp after the reaction would be

$$Ca : OH : Cl = 9.24 : 0.82 : 0.42.$$

Therefore,

$$OH : Cl = 0.82 : 0.42 \fallingdotseq 2 : 1.$$

That is, 1/3 of the amount of the OH groups in DAp must be exchanged by Cl. The IR absorbance decrease rate of the OH peak at 3570 cm^{-1} supports this conclusion.

Table 4. Cl/Ca Molar Ratio in Surface and Bulk Portions of DAp by EDX

	Cl/Ca molar ratio	
Sample	Surface	Bulk
DAp reacted	0.08	0.07
Chloroapatite	—	0.20

According to the measurements of XRD and XPS, the basic apatitic structure of DAp scarcely varied. On the other hand, Cl was captured on or in DAp along with the catalytic decomposition of TCE. The observation of the Cl binding energy and its spectrum by XPS supports the idea that the Cl species on DAp after the reaction could be chloroapatite, $Ca_{10}(PO_4)_6Cl_2$.

Consequently, after the oxidative catalytic decomposition of TCE over DAp, HCl immediately formed reacts with DAp as follows:

$$HCl + DAp \rightarrow H_2O + Cl\text{-}DAp.$$

The authors are grateful to Mr. Tadao Wakabayashi of Shimadzu Techno Research for the XPS measurement.

References

1) S. Imamura, T. Ikeda, and S. Ishida, *Nippon Kagaku Kaishi*, 139 (1989).
2) D. Pope, D. S. Walker, and R. L. Moss, *Atmos. Environ.*, **10**, 951 (1976).
3) D. Pope, D. S. Walker, and R. L. Moss, *Atmos. Environ.*, **12**, 1921 (1978).
4) S. L. Hung and L. D. Pfefferle, *Environ. Sci. Technol.*, **23**, 1085 (1989).
5) H. Nishikawa and H. Monma, *Nippon Kagaku Kaishi*, 1562 (1991).
6) W. T. Reichle, *J. Catal.*, **17**, 297 (1970).
7) N. S. Figoli, H. R. Keselman, P. C. L'Argentiere, and C. L. Lazzaroni, *J. Catal.*, **77**, 64 (1982).
8) N. S. Figoli, H. R. Keselman, P. C. L'Argentiere, and C. L. Lazzaroni, *J. Catal.*, **85**, 538 (1984).
9) J. A. Bett, L. G. Christner, and W. K. Hall, *J. Am. Chem. Soc.*, **89**, 5535 (1967).
10) H. Monma, *J. Catal.*, **75**, 200 (1982).
11) N. Hitmi, C. LaCabanne, and R. A. Young, *J. Phys. Chem. Solids*, **49**, 541 (1988).
12) "NIST X-Ray Photoelectron Spectroscopy Database," U. S. Department of Commerce, NIST, 1989.
13) H. Monma, S. Ueno, M. Tsutsumi, and T. Kanazawa, *Yogyo Kyokai Shi*, **86**, 28 (1978).